CHAPTER 4

Myocardial Denervation Coincides with Scar Heterogeneity in Ischemic Cardiomyopathy: a PET and CMR study

JOURNAL OF NUCLEAR CARDIOLOGY. 2015 NOV, EPUB AHEAD OF PRINT.

Stefan de Haan

Mischa T. Rijnierse

Hendrik J. Harms

Hein J. Verberne

Adriaan Lammertsma

Marc C. Huisman

Albert D. Windhorst

Albert C. van Rossum

Cornelis P. Allaart

Paul Knaapen

ABSTRACT

Background: Mismatch between myocardial innervation and perfusion assessed with positron emission tomography (PET) is a potential risk marker for ventricular arrhythmias in patients with ischemic cardiomyopathy. This mismatch zone originates from residual viable myocardium that has sustained ischemic nerve injury. Heterogenic scar size assessed with late gadolinium enhanced (LGE) cardiac magnetic resonance imaging (CMR) is also a risk marker of ventricular arrhythmias. These two imaging parameters may represent identical morphological tissue features. The current study explored the relation between innervation-perfusion mismatch and heterogenic scar size.

Methods: Twenty-eight patients (26 males, age 67±8 years) with ischemic cardiomyopathy and a left ventricular ejection fraction below 35%, eligible for ICD implantation were included. All patients underwent both [^{11}C]-hydroxyephedrine and [^{15}O]-water PET studies to assess myocardial sympathetic innervation and perfusion. LGE CMR was conducted to assess total myocardial scar size, scar core size, and heterogenic scar size.

Results: Perfusion defect size was 16.6±9.9% and innervation defect size was 33.7±10.8%, which resulted in an innervation-perfusion mismatch of 17.6±8.9%. Total scar size, scar core size, and heterogenic scar size were 21.2±8.6%, 14.7±6.6%, and 6.5±2.9%, respectively. No relation between scar core size and perfusion deficit size was observed ($r=0.18$, $p=0.36$). Total scar size was correlated with the innervation defect size ($r=0.52$, $p=0.004$) and the heterogenic scar zone displayed a significant correlation with the innervation-perfusion mismatch area ($r=0.67$, $p<0.001$).

Conclusions: Denervated residual viable myocardium in ischemic cardiomyopathy as observed with innervation-perfusion PET is related to the heterogenic scar zone as assessed with LGE CMR.

INTRODUCTION

Implantable cardioverter defibrillators (ICDs) have been shown to reduce mortality in patients at risk of sudden cardiac death.[1,2] However, a substantial proportion of patients do not receive an appropriate ICD therapy, yet are at risk of device related complications.[3] Therefore, numerous suggestions have been made to optimize selection criteria for implantation.[4-6] Studies have been focusing on myocardial scar characteristics assessed with late gadolinium enhanced (LGE) cardiac magnetic resonance imaging (CMR) as potential risk stratifiers of sudden cardiac death.[7-9] One of these characteristics is the heterogenic scar zone, which is hypothesized to consist of an admixture of vital myocytes and fibrosis. Ventricular tachycardias may originate in this zone due to the presence of electrical micro re-entry circuits. Indeed, several studies have linked the size of the heterogenic scar zone to the occurrence of ventricular tachycardias and sudden cardiac death.[8-11]

Alternatively, myocardial denervation may also contribute to electrical instability and propagate ventricular tachycardias after myocardial ischemia.[12] Cardiac nerves have been shown to be more vulnerable to ischemia and, therefore, the area of denervation is frequently of greater magnitude as compared to the infarct size.[12-15] This penumbra therefore consists of viable myocardium with impaired innervation. Positron emission tomography (PET) can accurately assess both myocardial scar as well as innervation. As such, the viable denervated peri-infarct zone can be visualized and has been linked to altered conduction and occurrence of ventricular tachycardias in animal experiments.[14,16]

From a pathophysiological point of view, both imaging techniques with LGE-CMR and PET may actually discern the identical phenomenon. Studies that have compared these imaging parameters in patients with ischemic cardiomyopathy are, however, lacking. The current pilot study was conducted to evaluate the penumbra adjacent to the infarct area with LGE-CMR and PET and attempt to link the magnitude of this area to the inducibility of ventricular arrhythmias.

METHODS

Study population

Twenty-eight patients with ischemic cardiomyopathy and a left ventricular ejection fraction below 35%, who were eligible for ICD implantation for primary prevention, were included in the current study. In all patients myocardial ischemia and viability were ruled out or coronary anatomy was not amendable for further revascularization. All patients were in a stable clinical condition. Patients with contraindications for PET or CMR (e.g. pacemaker, claustrophobia, irregular heart rhythm) were excluded. The study was approved by the institutional Medical Ethics Review Committee and all participants gave written informed consent prior to inclusion.

PET/CT acquisition

All studies were performed on a Gemini TF-64 PET/CT scanner (Philips Healthcare, Best, The Netherlands).[17] For perfusion imaging, a 5 mL bolus injection (0.8 ml·s^{-1}) of 370 MBq [^{15}O]-water followed by a 35 ml saline flush (2 ml·s^{-1}) was administered simultaneously with the start of a list-mode emission scan of 6 minutes. Immediately after the emission scan, a respiration-averaged CT scan was acquired (30 mAs, rotation time 1.5 s, pitch 0.825, collimation 16x0.625, covering 20 cm in 37 s during normal breathing) to correct for attenuation. The emission scan was reconstructed into 22 frames (1x10, 8x5, 4x10, 2x15, 3x20, 2x30 and 2x60 s) using the 3D row action maximum likelihood algorithm (3D RAMLA) and applying all appropriate corrections for scanner normalization, dead time, decay, scatter, randoms and attenuation. Subsequently, innervation imaging was conducted with [^{11}C]-hydroxyephedrine (HED), which was synthesized as described previously.[18] 370 MBq [^{11}C]-HED was injected as a 5 ml bolus (0.8 ml·s^{-1}) followed by a 35 ml saline flush (2 ml·s^{-1}), simultaneously starting a 60 min list-mode emission scan. Again, emission acquisition was followed by a CT scan to correct for attenuation. All patients received a radial artery catheter for arterial blood sampling during the dynamic scan. 7ml arterial samples were collected manually at 2.5, 5, 10, 20, 30, 40 and 60 minutes after administration of [^{11}C]-HED. Activity concentrations in plasma and whole blood were determined in each sample as described previously.[18] Emission images were reconstructed into 36 frames (1 x 10 s, 8 x 5s, 4 x 10 s, 3 x 20 s, 5 x 30 s, 5 x 60 s, 4 x 150 s, 4 x 300 s, 2 x 600 s).

PET/CT image analysis

In-house developed software was used to obtain input functions. One cm diameter regions of interest (ROIs) were placed over the ascending aorta in at least 5 transaxial image planes in the frame showing the first pass of the injected bolus. These ROIs were combined in one volume of interest (VOI) for the ascending aorta. A second set of ROIs was placed over the right-ventricular (RV) cavity in 5 transaxial planes, with ROI boundaries at least 1 cm from the RV wall to avoid spill-over of myocardial activity. Again these ROIs were combined in a VOI for the RV-cavity. Both VOIs were then transferred to the full dynamic images to obtain arterial whole blood and RV time-activity curves (TACs). For [^{11}C]-HED metabolite correction was performed using the arterial samples. Subsequently, seventeen myocardial segment VOIs were drawn manually on the final frame of the dynamic scan for [^{11}C]-HED and on parametric perfusable tissue fraction images for [^{15}O]-water according to the 17-segment model of the American Heart Association.[19] This VOI template was projected onto the entire emission scan to extract segmental TACs. Segment TACs were fitted to a single tissue compartment model for both [^{15}O]-water and [^{11}C]-HED as described previously.[20] Myocardial blood flow (MBF) was multiplied by the perfusable tissue index to obtain transmural perfusion values (MBF_T). To minimize the effect of global reduction of innervation of the myocardium due

to heart failure on the innervation defect, defect sizes were normalized to a reference area of remote myocardium. In all patients four myocardial segments remote of scar were designated as the reference area. Subsequently, perfusion and innervation defect sizes were calculated at different cut-off percentages of the mean of the reference segments. Optimum cut-off was defined as the cut-off percentage at which innervation and perfusion mismatch was largest. Innervation and perfusion mismatch was defined as the difference between HED defect size and MBF_T defect size.

CMR image acquisition

CMR studies were performed on a 1.5 Tesla whole body scanner (Magnetom Sonata or Avanto, Siemens, Erlangen, Germany), using a six-channel phased-array body coil. After survey scans, a retro-triggered, balanced steady-state free precession gradient-echo sequence was used for cine imaging. Image parameters included slice thickness of 5 mm, slice gap 5 mm, temporal resolution <50 ms, repetition time 3.2 ms, echo time 1.54 ms, flip angle 60° and a typical image resolution of 1.3 x 1.6 x 5.0 mm. The cardiac cycle consisted of 20 phases. After obtaining 4-, 3- and 2-chamber view cines, stacks of 10 to 12 short axis slices were acquired to fully cover the LV. Cine images were acquired during breath-hold at mild expiration. Subsequently, 10 to 15 minutes after administration of 0.2 $mmol \cdot kg^{-1}$ gadolinium-DTPA contrast images were acquired in the same views as in the cine images, using a two-dimensional segmented inversion-recovery prepared gradient echo sequence (TE 4.4 ms, TR 9.8 ms, inversion time 250 to 300 ms, typical voxel size $1.3 \times 1.6 \times 5.0\ mm^3$).

CMR image analysis

Images were analysed off-line using the software package MASS (MR Analytical Software System, Medis, Leiden, The Netherlands). To analyse left ventricular volumes, endocardial and epicardial borders of the left ventricle were outlined manually in both end-diastolic and end-systolic phases of all short axis images. Papillary muscles were included in the left ventricular volume. End-diastolic volume (EDV), end-systolic volume (ESV), and ejection fraction (EF) were computed using these analyses. Subsequently, endocardial and epicardial contours of the late gadolinium enhanced (LGE) images were traced manually. Total scar size, scar core size and heterogenic scar zone size were calculated using the full width halve max (FWHM) method, which defines scar core as myocardium with signal intensity ≥ 50% of the maximum signal intensity of the hyperenhanced area. The heterogenic scar zone is defined as myocardium with signal intensity between 35% and 50% of maximum signal intensity.[9] Total scar size is defined as the total of scar core size and heterogenic scar zone size. All areas of enhancement were quantified by computer assisted planimetry on each of the short axis images and expressed as percentage of myocardium.

Electrophysiological testing

All patients were implanted with an ICD and during implantation electrophysiological testing was performed. The stimulation protocol was carried out through the ICD and consisted of two basic 8-beat drive trains with cycle lengths of 600 and 400 ms, followed by up to three extrastimuli at different cycle lengths delivered from the right ventricular lead. Positive electrophysiological testing was defined as the induction of a sustained monomorphic ventricular tachycardia that lasted ≥30 seconds or required cardioversion for hemodynamic compromise.

Statistical Analysis

Continuous variables are presented as mean ± SD, and categorical data are summarized as frequencies and percentages. For comparison of two data sets, paired and unpaired Student's t-test was used when appropriately. Levene's Test for Equality of Variances was used to verify if the application of the unpaired Student's t-test was appropriate. Correlation between two data sets was calculated using the Pearson correlation test. A value of $P < 0.05$ was considered statistically significant. The statistical analysis was performed by means of SPSS for Windows (version 16.0, SPSS Inc., Chicago, USA).

RESULTS

Twenty-eight patients were included in current study. Baseline characteristics of these patients are listed in table 1. Figure 1 shows a typical example of a patient with an anterior myocardial infarction. These polarmaps show similar infarct regions, and similar perfusion-innervation mismatch and heterogenic scar zone areas.

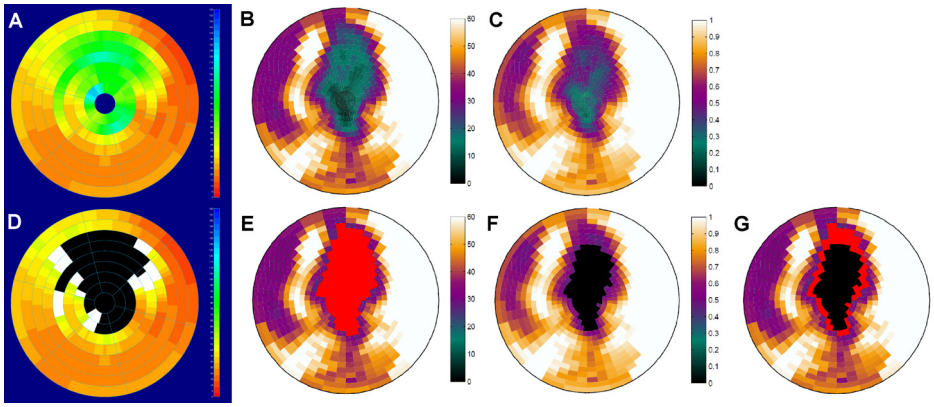

Figure 1. Example of a patient with an anterior myocardial infarction. Panel A: Polarmap of LGE CMR signal intensity; panel B: HED polarmap; panel C: MBF polarmap. Panel D: LGE CMR polarmap with scar core indicated in black and heterogenic scar zone indicated in white; panel E: HED defect size indicated in red; panel F: MBF defect size indicated in black; panel G: innervation and perfusion mismatch area indicated in red (HED defect size minus MBF defect size).

Table 1. Characteristics of study population (n = 28).

Patient characteristics (n = 28)	Mean ± SD or N (%)
Age (y)	66.8 ± 8.1
Male gender, n (%)	26 (93%)
Coronary risk profile, n (%)	
Diabetes Mellitus type II	5 (18%)
Hypertension	11 (39%)
Hypercholesterolemia	9 (32%)
Smoking history	14 (50%)
Medication, n (%)	
Antiplatelet therapy	28 (100%)
β-blockers	27 (96%)
ACE-I or ARB	26 (93%)
Ca channel blocker	3 (11%)
Amiodarone	1 (4%)
Statin	25 (89%)
Diuretics	14 (50%)
Medical history, n (%)	
PCI/CABG	16/14 (57%/50%)
NYHA class I/II/III	8/17/3 (28/61/11%)
Serologic markers,	
NT-pro-BNP (ng/L)	1685 ± 2942
Creatinine (μmol/L)	92 ± 29

ACE, angiotensin converting enzyme; ARB, angiotensin-II-receptor blockers; Ca, calcium; CAD, coronary artery disease; CABG, coronary arterial bypass graft surgery; NT-proBNP, N-terminal prohormone of brain natriuretic peptide; NYHA, New York Heart Association; PCI, percutaneous coronary intervention.

CMR and PET parameters

CMR and PET imaging are shown in table 2. Left ventricular ejection fraction was 29 ± 7%. Total scar size was 21.2 ± 8.6% with a scar core size of 14.7 ± 6.6%, which resulted in a heterogenic scar zone size of 6.5 ± 2.9% Results of PET imaging are presented in table 2. Global MBF at rest was 0.67 ± 0.14 ml·min^{-1}·g^{-1} and global innervation was 26.4 ± 18.8 mL·g^{-1}. Defect sizes of both MBF and HED were calculated at different cut-offs and the innervation and perfusion mismatch was derived for different cut-offs as described (Figure 2). A cut-off of 50% of the mean of the remote area yielded the largest mismatch between innervation and perfusion. Therefore, the 50% cut-off was used to define defect sizes. These cut-offs resulted in a perfusion defect size of 16.6 ± 9.9% and an innervation defect size of 33.7 ± 10.8%. Consequently, the innervation-perfusion mismatch was 17.6 ± 8.9%.

Table 2. Imaging parameters (n = 28).

Imaging parameters (n = 28)	Mean ± SD
CMR parameters	
EDV (mL)	263 ± 62
ESV (mL)	188 ± 53
EF (%)	29 ± 7
Scar core size (%)	14.7 ± 6.6
Total scar size (%)	21.2 ± 8.6
Heterogenic scar zone (%)	6.5 ± 2.9
PET/CT parameters	
Perfusion (MBF) (mL·min^{-1}·g^{-1})	0.68 ± 0.14
Innervation (HED) (mL·g^{-1})	26.4 ± 18.8
Perfusion in healthy segments (MBF) (mL·min^{-1}·g^{-1})	0.78 ± 0.13
Innervation in healthy segments (HED) (mL·g^{-1})	29.3 ± 17.2
Perfusion (MBF) defect (%)	16.6 ± 9.9
Innervation (HED) defect (%)	33.7 ± 10.8
Innervation-perfusion mismatch (%)	17.6 ± 8.9

CMR: cardiac magnetic resonance imaging; HED: hydroxyepinephrine; MBF: myocardial blood flow • perfusable tiswsue index.

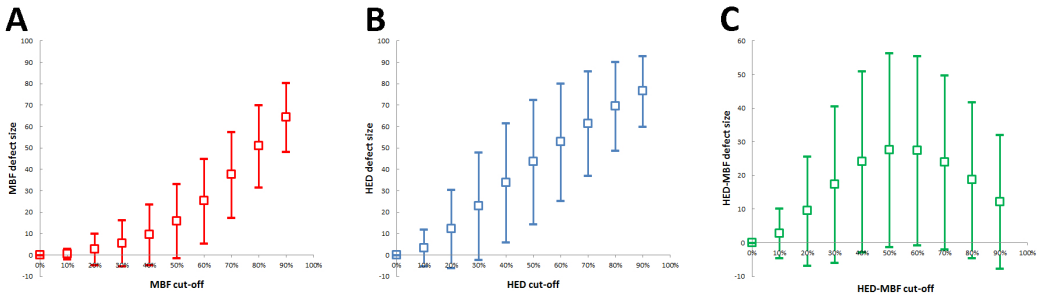

Figure 2. Defect sizes according to different cut-offs. Panel A: MBF defect sizes; panel B: HED defect sizes; panel C: HED- MBF defect sizes; boxes: mean defect size with 2SD indicated.

CMR vs PET

Scar core size measured by LGE CMR was comparable to MBF defect size (p=0.50). However, no apparent correlation was seen between both parameters (r=0.18, p=0.36) (Figure 3). Innervation defect size was significantly larger than the mean total scar size (p<0.001) and correlated moderately (r=0.52, p=0.004) (Figure 3). Compared to the innervation-perfusion mismatch the heterogenic scar zone size was significantly smaller 6.5 ± 2.9% (p<0.001). Nevertheless, an evident correlation was found between heterogenic scar zone size and innervation-perfusion mismatch (r=0.67, p<0.001) (Figure 4).

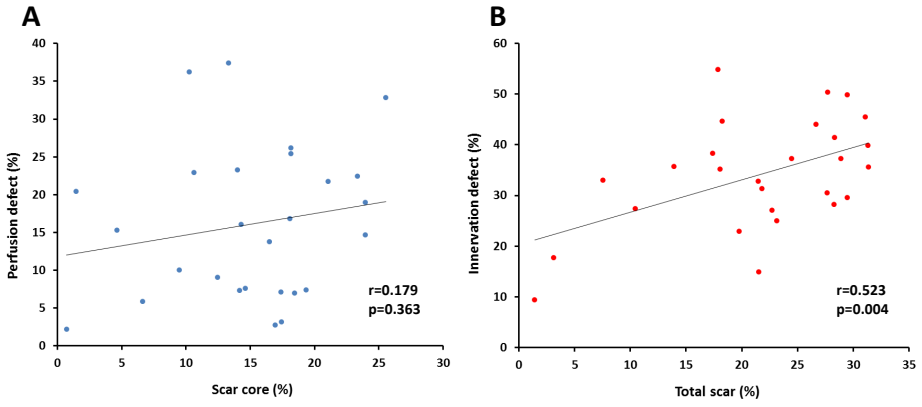

Figure 3. Panel A: Correlation of myocardial scar core size (%), assessed with LGE CMR, and MBF defect size (%), assessed with [^{15}O]-water PET; r=0.179; p=0.363. Panel B: Correlation of total myocardial scar size (%), assessed with LGE CMR, and innervation defect size (%), assessed with [^{11}C]-HED PET; r=0.523; p=0.004.

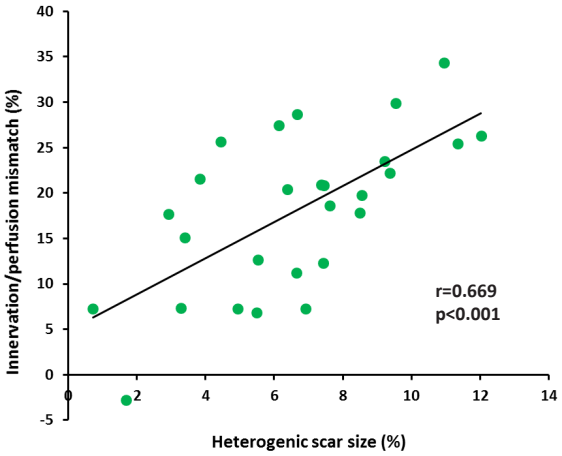

Figure 4. Correlation of innervation and perfusion mismatch, assessed with [^{11}C]-HED and [^{15}O]-water PET, and heterogenic scar zone, assessed with LGE CMR; r=0.669; p<0.001.

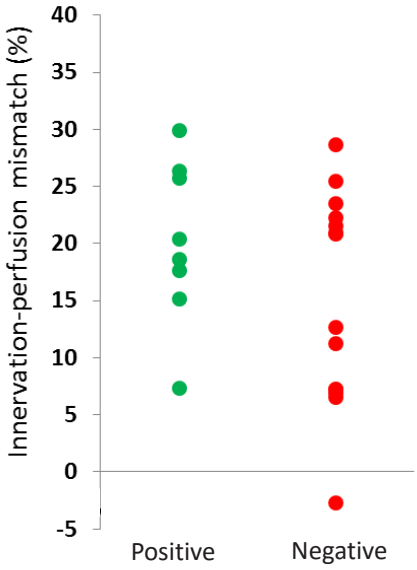

Figure 5. Distribution of innervation and perfusion mismatch, assessed with [^{11}C]-HED and [^{15}O]-water, according to inducibility of monomorphic ventricular tachycardia on electrophysiological testing (positive: monomorphic VT inducible; negative: monomorphic VT not inducible), p=0.208.

Electrophysiological testing

Of the 28 included patients 22 underwent electrophysiological testing. One patient withdrew consent for the electrophysiological testing procedure, 1 patient did not underwent electrophysiological testing due to technical problems, and in 4 patients the procedure was cancelled due to the presence of micro thrombi in the left ventricle on LGE CMR. A monomorphic sustained ventricular tachycardia was induced in 8 patients. The innervation-perfusion mismatch in patients in whom monomorphic ventricular tachycardias were inducible was 20.1 ± 7.2% whereas patients who were not inducible displayed a mismatch of 15.2 ± 9.3%. However, this difference was not significant (p=0.21) (Figure 5). Inducible and non-inducible patients were compared for all remaining CMR and PET parameters and none of these parameter significantly differed between both groups (Table 3).

Table 3. Differences in imaging parameters between patients who are inducible and non-inducible at electrophysiological study (n = 22).

Imaging parameters (n = 22)	Inducible patients (n=8) Mean ± SD	Non-inducible patients (n=14) Mean ± SD	P-value
CMR parameters			
EDV (mL)	249 ± 46	275 ± 68	0.372
ESV (mL)	173 ± 26	202 ± 62	0.233
EF (%)	30 ± 7	28 ± 7	0.432
Scar core size (%)	13.9 ± 5.0	14.4 ± 7.9	0.889
Total scar size (%)	20.1 ± 7.0	20.4 ± 10.1	0.956
Heterogenic scar zone (%)	6.2 ± 3.1	6.0 ± 2.9	0.871
PET/CT parameters			
Perfusion (MBF) ($mL \cdot min^{-1} \cdot g^{-1}$)	0.70 ± 0.21	0.67 ± 0.11	0.657
Innervation (HED) ($mL \cdot g^{-1}$)	26.9 ± 19.1	22.5 ± 12.8	0.628
Perfusion (MBF) defect (%)	17.2 ± 10.1	15.6 ± 10.0	0.740
Innervation (HED) defect (%)	37.4 ± 7.2	30.8 ± 11.0	0.166
Innervation-perfusion mismatch (%)	20.1 ± 7.2	15.2 ± 9.3	0.208

CMR: cardiac magnetic resonance imaging; HED: hydroxyepinephrine; MBF: myocardial blood flow • perfusable tissue index

DISCUSSION

The current study was conducted to evaluate whether the heterogenic scar characteristics adjacent to an infarct zone as observed with LGE CMR coincided with denervated, yet viable, myocardium as visualized with PET. Indeed, the magnitude of the innervation-perfusion mismatch zone was correlated with the size of the heterogenic scar zone as measured with LGE CMR. These imaging characteristics did not appear to be related to the inducibility of ventricular arrhythmias.

Several studies have shown an association of ventricular arrhythmias with their substrates, such as scar size, perfusion and innervation.[6-12,15] However, none of them looked at the correlation between the different substrates. This study was the first to compare scar characteristics with myocardial innervation and perfusion. Current results of the LGE CMR assessment are in line with previous studies. Mean size of scar core, total scar, and heterogenic scar zone are comparable to earlier studies,[8-11] albeit those studies demonstrated a relationship between scar parameters and ventricular arrhythmias. The inability of the current study to demonstrate a relation between scar parameters and the inducibility of ventricular arrhythmias might be due to the small sample size. Furthermore, studies utilized varying methods and cut-off values for the assessment of scar characteristics. These differences will influence the results, but a previous study showed that the predictive value of the different methods for ventricular arrhythmias are comparable.[8]

Sasano et al. showed the feasibility of assessment of cardiac innervation and perfusion with PET in a pig model.[12] The presence of the mismatch between innervation and perfusion has been confirmed in humans with SPECT and, recently, the mismatch was assessed with PET in the PAREPET-study.[14,15] The current data also display the feasibility of both innervation and perfusion imaging with PET in humans. However, perfusion was assessed with [^{15}O]-water in current study whereas the PAREPET-study used [^{13}N]-ammonium. Perfusion data are similar as seen in prior studies and, also innervation defect results are similar to previous studies.[6, 15] Although different analysis methods and, consequently, different cut-offs for determination of perfusion and innervation defect sizes were used. Current study did not show a correlation between scar size measured with LGE CMR and perfusion defect assessed with PET. An important factor which influences this correlation is the presence of hibernating myocardium. All patients underwent revascularization when possible, which not means that patients are completely revascularized. Some patients will have hibernating myocardium with a reduced perfusion. Previous studies have shown a relation between presence of scar and measured flow, but no correlation between scar size measured by LGE CMR and perfusion defect has been described. [21,22]

The demonstrated correlation between innervation and perfusion mismatch and heterogenic scar size might be the result of a common origin, i.e. limited ischemia. Previous

studies have shown that the innervation of the myocardium is more vulnerable to ischemia than myocytes.[12-15] As a result, denervation is present in areas of limited ischemia, but myocytes remain intact in the same areas of limited ischemia. This results in areas of mismatch between innervation and perfusion, which are predominantly found in the border zone of a myocardial infarction, where limited ischemia is most likely. Heterogenic scar also arises in these areas of limited ischemia, which results in areas composed of both fibrosis and preserved myocytes. Due to this mixed composition, the peri-infarct zone displays an intermediate signal intensity on LGE images that is higher than normal myocardium, but lower than the infarct core.[23] The current study showed a clear correlation between innervation and perfusion mismatch and the heterogenic scar zone size. However, both entities are not interchangeable, since the innervation and perfusion mismatch area is consistently larger compared to the heterogenic scar size. An important explanation for the larger innervation and perfusion mismatch is the higher vulnerability of innervation for ischemia.[13]

Several studies have been conducted that focused on cardiac innervation. All studies showed a larger innervation defect as a result of ischemia compared to the perfusion defect,[12-15] which was confirmed in the current study. This mismatch between innervation and perfusion has been associated with conduction abnormalities and ventricular tachycardias. Calkins et al. demonstrated that the refractory period of the myocardium was larger in denervated areas, which makes them possibly more arrhythmogenic.[16] Furthermore, Simoes et al. showed a correlation between innervation and perfusion mismatch size and prolonged repolarization.[14] Subsequently, in a pig model it was affirmed that larger areas of mismatch between innervation and perfusion are correlated to ventricular tachycardias induced at electrophysiological testing and the induced ventricular tachycardias originated from the mismatch areas.[12] This correlation could not be confirmed in humans in a SPECT study using [^{123}I]mIBG and [^{99m}Tc]tetrofosmin,[24] in which a crude parameter for innervation and perfusion mismatch was used, which might have hampered the assessment of the association. Nonetheless the study did show a predictive value of a diminished global innervation. The ADMIRE-HF study also showed in a large population a clear predictive value of global diminished myocardial innervation for ventricular tachycardias and sudden cardiac death.[25] However, there was no assessment of myocardial perfusion in the ADMIRE-HF study reported and, consequently, there was no assessment of innervation and perfusion mismatch. Fallavollita et al. showed that the innervation defect size is an independent predictor of sudden cardiac death in ischemic cardiomyopathy patients.[15] They also assessed myocardial perfusion, though innervation perfusion mismatch did not appear to be an independent predictor of sudden cardiac death. This study could not demonstrate a relation between innervation and perfusion mismatch and inducibility of ventricular tachycardias. Furthermore, no relation was observed between global innervation defect size and inducibility of ventricular tachycardias. This dissimilarity might be due to method-

ological discrepancies between studies and a sample size too small to reveal significant differences. Additionally, there is not a standard cut-off value to determine innervation and perfusion defect sizes. All previous studies used varying cut-off values, which might have an important impacted on the defect size and predictive values for ventricular arrhythmias.[12,15] In contrast to these studies, the optimal cut-off value to provide the largest innervation - perfusion defect size was explored. The optimal cut-off was at 50% of normal remote myocardium. Furthermore, innervation was assessed quantitatively, which may give a more accurate estimation of innervation and, therefore, of the innervation defect size.

Limitations

Some limitations of the current study have to be addressed. First, image resolution of CMR Is superior to PET. Such differences might influence the results. Additionally, partial volume effects play a role in both imaging modalities and will affect the assessment of innervation, perfusion, and scar characteristics. Secondly, electrophysiological testing is used as a substitute of sudden cardiac death. Although there is an association between inducibility of monomorphic ventricular tachycardias during electrophysiological testing and sudden cardiac death, the positive predictive value of inducibility of monomorphic ventricular tachycardias for sudden cardiac death is low.[26,27] Finally, as already alluded to, the sample size was too small to draw definite conclusions. The small sample size was partly caused by the fact that some patients included in the study were not able to underwent electrophysiological testing.

Conclusion

In conclusion, current study shows the feasibility of assessment of both cardiac innervation and perfusion by PET with [^{11}C]-HED and [^{15}O]-water respectively in humans. Furthermore, mismatch between cardiac innervation and perfusion was shown to correlate with heterogenic scar size assessed with LGE CMR. However, both heterogenic scar size as well as innervation and perfusion mismatch did not relate to inducibility of monomorphic ventricular tachycardias. Future studies should focus on the potential of innervation and perfusion mismatch as risk marker of ventricular tachycardias and sudden cardiac death in larger study populations.

REFERENCES

1. Bardy GH, Lee KL, Mark DB, Poole JE, Packer DL, Boineau R et al. Amiodarone or an implantable cardioverter-defibrillator for congestive heart failure. *N Engl J Med* 2005;352:225-37.

2. Moss AJ, Zareba W, Hall WJ, Klein H, Wilber DJ, Cannom DS et al. Prophylactic implantation of a defibrillator in patients with myocardial infarction and reduced ejection fraction. *N Engl J Med* 2002;346:877-83.

3. Moss AJ, Greenberg H, Case RB, Zareba W, Hall WJ, Brown MW et al. Long-term clinical course of patients after termination of ventricular tachyarrhythmia by an implanted defibrillator. *Circulation* 2004;110:3760-5.

4. Buxton AE, Lee KL, Hafley GE, Pires LA, Fisher JD, Gold MR et al. Limitations of ejection fraction for prediction of sudden death risk in patients with coronary artery disease: lessons from the MUSTT study. *J Am Coll Cardiol* 2007;50:1150-7.

5. de Haan S, Knaapen P, Beek AM, de Cock CC, Lammertsma AA, van Rossum AC et al. Risk Stratification for Ventricular Arrhythmias in Ischemic Cardiomyopathy: the value of non-invasive imaging. *Europace* 2010;12:468-74.

6. Rijnierse MT, de Haan S, Harms HJ, Robbers LF, Wu L, Danad I et al. Impaired hyperemic myocardial blood flow is associated with inducibility of ventricular arrhythmia in ischemic cardiomyopathy. *Circ Cardiovasc Imaging* 2014;7:20-30.

7. Bello D, Fieno DS, Kim RJ, Pereles FS, Passman R, Song G et al. Infarct morphology identifies patients with substrate for sustained ventricular tachycardia. *J Am Coll Cardiol* 2005;45:1104-8.

8. de Haan S, Meijers TA, Knaapen P, Beek AM, van Rossum AC, Allaart CP. Scar size and characteristics assessed by CMR predict ventricular arrhythmias in ischaemic cardiomyopathy: comparison of previously validated models. *Heart* 2011 December; 97(23):1951-6.

9. Roes SD, Borleffs CJW, van der Geest RJ, Westenberg JJ, Marsan NA, Kaandorp TA et al. Infarct tissue heterogeneity assessed with contrast-enhanced MRI predicts spontaneous ventricular arrhythmia in patients with ischemic cardiomyopathy and implantable cardioverter-defibrillator. Circulation: *Cardiovascular Imaging* 2009;2: 183-90.

10. Schmidt A, Azevedo CF, Cheng A, Gupta SN, Bluemke DA, Foo TK et al. Infarct tissue heterogeneity by magnetic resonance imaging identifies enhanced cardiac arrhythmia susceptibility in patients with left ventricular dysfunction. *Circulation* 2007;115:2006-14.

11. Yan AT, Shayne AJ, Brown KA, Gupta SN, Chan CW, Luu TM et al. Characterization of the peri-infarct zone by contrast-enhanced cardiac magnetic resonance imaging is a powerful predictor of post-myocardial infarction mortality. *Circulation* 2006; 114:32-9.

12. Sasano T, Abraham MR, Chang KC, Ashikaga H, Mills KJ, Holt DP et al. Abnormal sympathetic innervation of viable myocardium and the substrate of ventricular tachycardia after myocardial infarction. *J Am Coll Cardiol* 2008;51:2266-75.

13. Bulow HP, Stahl F, Lauer B, Nekolla SG, Schuler G, Schwaiger M et al. Alterations of myocardial presynaptic sympathetic innervation in patients with multi-vessel coronary artery disease but without history of myocardial infarction. *Nucl Med Commun* 2003;24:233-9.

14. Simoes MV, Barthel P, Matsunari I, Nekolla SG, Schömig A, Schwaiger M et al. Presence of sympathetically denervated but viable myocardium and its electrophysiologic correlates after early revascularised, acute myocardial infarction. *Eur Heart J* 2004;25:551-7.

15. Fallavollita JA, Heavey BM, Luisi AJ Jr, Michalek SM, Baldwa S, Mashtare TL Jr et al. Regional myocardial sympathetic denervation predicts the risk of sudden cardiac arrest in ischemic cardiomyopathy. *J Am Coll Cardiol* 2014; 63:141-9.

16. Calkins H, Allman K, Bolling S, Kirsch M, Wieland D, Morady F et al. Correlation between scintigraphic evidence of regional sympathetic neuronal dysfunction and ventricular refractoriness in the human heart. *Circulation* 1993;88:172-9.

17. Surti S, Kuhn A, Werner ME, Perkins AE, Kolthammer J, Karp JS. Performance of Philips Gemini TF PET/CT scanner with special consideration for its time-of-flight imaging capabilities. *J Nucl Med* 2007;48:471-80.

18. Harms HJ, de Haan S, Knaapen P, Allaart CP, Rijnierse MT, Schuit RC et al. Quantification of [11C]-meta-hydroxyephedrine uptake in human myocardium. *EJNMMI Research* 2014;4:52-63.

19. Cerqueira MD, Weissman NJ, Dilsizian V, Jacobs AK, Kaul S, Laskey WK et al. Standardized myocardial segmentation and nomenclature for tomographic imaging of the heart. A statement for healthcare professionals from the Cardiac Imaging Committee of the Council on Clinical Cardiology of the American Heart Association. *Circulation* 2002;105:539-42.

20. Boellaard R, Knaapen P, Rijbroek A, Luurtsema GJ, Lammertsma AA. Evaluation of basis function and linear least squares methods for generating parametric blood flow images using 15O-water and Positron Emission Tomography. *Mol Imaging Biol* 2005;7:273-85.

21. Knaapen P, Bondarenko O, Beek AM, Götte MJ, Boellaard R, van der Weerdt AP, et al. Impact of scar on water-perfusable tissue index in chronic ischemic heart disease: evaluation with PET and contrast-enhanced MRI. *Mol Imaging Biol.* 2006;8:245–51.

22. de Haan S, Harms HJ, Lubberink M, Allaart CP, Danad I, Chen WJY, Diamant M, van Rossum AC, Iida H, Lammertsma AA, Knaapen P. Parametric imaging of myocardial viability using 15O-labelled water and PET/CT: comparison with late gadolinium-enhanced CMR. *Eur J Nucl Med Mol Imaging.* 2012;39:1240–1245.

23. Schelbert EB, Hsu LY, Anderson SA, Mohanty BD, Karim SM, Kellman P et al. Late gadolinium-enhancement cardiac magnetic resonance identifies postinfarction myocardial fibrosis and the border zone at the near cellular level in ex vivo rat heart. *Circ Cardiovasc Imaging* 2010;3:743-52.

24. Bax JJ, Kraft O, Buxton AE, Fjeld JG, Parízek P, Agostini D et al. 123I-mIBG Scintigraphy to Predict Inducibility of Ventricular Arrhythmias on Cardiac Electrophysiology Testing: A Prospective Multicenter Pilot Study. *Circulation: Cardiovascular Imaging* 2008;1:131-40.

25. Jacobson AF, Senior R, Cerqueira MD, Wong ND, Thomas GS, Lopez VA et al. Myocardial Iodine-123 Meta-Iodobenzylguanidine Imaging and Cardiac Events in Heart Failure Results of the Prospective ADMIRE-HF (AdreView Myocardial Imaging for Risk Evaluation in Heart Failure) Study. *J Am Coll Cardiol* 2010;55:2212-21.

26. Bourke JP, Richards DA, Ross DL, Wallace EM, McGuire MA, Uther JB. Routine programmed electrical stimulation in survivors of acute myocardial infarction for prediction of spontaneous ventricular tachyarrhythmias during follow-up: results, optimal stimulation protocol and cost-effective screening. *J Am Coll Cardiol* 1991;18:780-8.

27. Richards DA, Byth K, Ross DL, Uther JB. What is the best predictor of spontaneous ventricular tachycardia and sudden death after myocardial infarction? *Circulation* 1991;83:756-63.